

Derandomized novelty detection with FDR control via conformal e-values

Meshi Bashari^{*1}, Amir Epstein², Yaniv Romano^{1,3}, and Matteo Sesia⁴

¹Department of Electrical and Computer Engineering, Technion IIT, Haifa, Israel

²Citi Innovation Lab, Tel Aviv, Israel

³Department of Computer Science, Technion IIT, Haifa, Israel

⁴Department of Data Sciences and Operations, University of Southern California, Los Angeles, California, USA

Abstract

Conformal prediction and other randomized model-free inference techniques are gaining increasing attention as general solutions to rigorously calibrate the output of any machine learning algorithm for novelty detection. This paper contributes to the field by developing a novel method for mitigating their algorithmic randomness, leading to an even more interpretable and reliable framework for powerful novelty detection under false discovery rate control. The idea is to leverage suitable conformal *e-values* instead of *p-values* to quantify the significance of each finding, which allows the evidence gathered from multiple mutually dependent analyses of the same data to be seamlessly aggregated. Further, the proposed method can reduce randomness without much loss of power, partly thanks to an innovative way of weighting conformal e-values based on additional side information carefully extracted from the same data. Simulations with synthetic and real data confirm this solution can be effective at eliminating random noise in the inferences obtained with state-of-the-art alternative techniques, sometimes also leading to higher power.

1 Introduction

1.1 Background and motivation

A common problem in statistics and machine learning is to determine which samples, among a collection of new observations, were drawn from the same distribution as a reference data set [43, 30, 13]. This task is known as *novelty detection*, *out-of-distribution testing*, or *testing for outliers*, and it arises in numerous applications within science, engineering, and business, including for example in the context of medical diagnostics [35], security monitoring [46], and fraud detection [6]. This paper looks at the problem from a model-free perspective, in the sense that it does not rely on parametric assumptions about the data-generating distributions, which are generally unknown and complex. Instead, we apply powerful machine learning models for one-class [26] or binary classification to score the new samples based on how they *conform* to patterns observed in the reference data, and then we leverage rigorous statistical arguments to translate such scores into reliable inferences.

The conformal inference framework [39, 21] provides flexible tools for extracting provably valid predictive inferences from any *black-box* model. The simplest implementation of conformal inference is based on random sample splitting. In the context of novelty detection, this consists of training a classifier on a subset of the reference data (possibly including some labeled outlier samples), and then ranking the output score for each test point against the corresponding scores evaluated out-of-sample for the hold-out reference data. As the latter only contain *inliers*, under relatively mild *exchangeability* assumptions the aforementioned rank can be proved to be uniformly distributed if the test point was sampled exchangeably from the reference distribution [19, 33, 16]. In other words, this calibration procedure yields a conformal *p-value* that can be utilized to test for outliers while rigorously controlling the probability of making a *false discovery*—incorrectly labeling a test inlier as an “outlier”. Further, split-conformal inference produces only weakly dependent *p-values* for different test points [9], in such a manner as to enable exact control of the

^{*}Authors listed in alphabetical order.

expected proportion of false discoveries—the *false discovery rate* (FDR)—with the powerful Benjamini-Hochberg (BH) filter [11].

A limitation of split-conformal inference is that it is aleatory, in the sense that its results for a given data set are unpredictable because they depend on how the reference samples are randomly divided between the training and calibration subsets. Randomized methods may naturally cause some confusion [45], and they become especially problematic in the hands of incautious practitioners who may accidentally cherry-pick random seeds or over-tune free hyper-parameters, completely invalidating the final inferences. This paper addresses the issue by developing a principled method to powerfully aggregate conformal tests for outliers obtained with repeated splits of the same data set, while retaining provable control of the FDR. This problem is challenging because dependent p-values for the same hypothesis are generally difficult to aggregate without incurring into a significant loss of power [37, 40]. Further, rigorous FDR control is typically difficult to achieve when working with dependent p-values, such as those produced by conformal calibration methods that are less randomized compared to simple data-splitting [8]. In fact, more sophisticated conformal inference methods yield more complicated p-value dependencies, and controlling the FDR under general dependence tends to involve large losses in power [12] or expensive computations [14].

1.2 Related work

There already exist some model-free inference methods that can lead to (at least partially) derandomized conformal p-values. One approach is that of *full-conformal* inference [39], which includes the test point into the training set and does not involve data splitting. This method is not randomized in the sense of split-conformal inference, but it is expensive because it requires completely re-training the machine learning model for every new test point. A more computationally efficient alternative is *K-fold cross-validation+* [8], which trains a fixed number of models (e.g., $K = 10$) and separately utilizes different subsets of the available data as hold-out calibration set. This naturally produces less aleatory inferences compared to standard split-conformal inference, and it has the additional advantage of being able to leverage potentially more powerful models trained on larger samples. For example, 90% of the available data points can be utilized for model training when the number of folds is 10. Yet, cross-validation+ does not fully resolve the problem considered in this paper for two reasons. First, it produces mutually dependent p-values for different test points that do not necessarily allow rigorous FDR control with the BH filter, due to a more complicated dependence structure compared to that of split-conformal p-values [9]. This issue could be tackled without excessive loss of power by replacing the BH procedure with the more flexible conditional FDR filtering strategy of Fithian and Lei [14], but that solution would be too computationally expensive to be feasible in large-scale applications [22]. Second, while cross-validation+ can mitigate randomness due to data splitting, it does not address other important sources of unpredictable algorithmic variability such as model initialization and hyper-parameter tuning, nor does it allow the principled aggregation of potentially inconsistent results based on different choices of machine learning models (e.g., neural networks vs. random forests). By contrast, the method proposed in this paper can be generally useful for aggregating conformal inferences and mitigating all aforementioned sources of randomness while provably controlling the FDR and attaining reasonably high power.

This paper builds upon *e-values* [38], quantitative measures of statistical evidence alternative to p-values that lend themselves particularly well to the derandomization of data-splitting procedures and to FDR control under dependence [41]. In particular, the novel method developed here is inspired by the recent work of Ren and Barber [28] on the derandomization of the knockoff filter [7] in the different context of high-dimensional variable selection. Further, our method borrows and re-purposes *transductive* [36] conformal inference ideas to leverage information contained in the test data themselves while calibrating the conformal inferences, boosting the power to detect outliers similarly to Marandon et al. [25] and Liang et al. [22].

Finally, it should be mentioned that several prior works have studied how to stabilize conformal predictors by efficiently calibrating the output of an *ensemble* of simpler models using scores evaluated *out-of-bag* [24, 10, 23, 18, 17]. However, the problem considered in this paper is clearly distinct as we focus on derandomizing existing conformal novelty detection methods while rigorously controlling the FDR over many test points.

2 Relevant technical background

2.1 Notation and problem setup

Consider a data set containing n observations, $X_i \in \mathbb{R}^d$, sampled exchangeably (or, for simplicity, independent and identically distributed) from some unknown distribution P_0 , for all $i \in \mathcal{D} = [n] = \{1, \dots, n\}$. Imagine then observing a test set of n_{test} “unlabeled” samples $X_j \in \mathbb{R}^d$. The problem studied in this paper is that of testing, for each $j \in \mathcal{D}_{\text{test}} = [n + n_{\text{test}}] \setminus [n]$, the *null hypothesis* that X_j is also an *inlier*, in the sense that it was randomly sampled from P_0 exchangeably with the data in \mathcal{D} . We refer to a rejection of this null hypothesis as the *discovery* that X_j is an *outlier*, and we indicate the set of true inlier test points as $\mathcal{D}_{\text{test}}^{\text{null}}$, with $n_{\text{test}}^{\text{null}} = |\mathcal{D}_{\text{test}}^{\text{null}}|$. For each $j \in \mathcal{D}_{\text{test}}$, define R_j as the binary indicator of whether X_j is labeled by our method as an outlier. Then, the goal is to discover as many true outliers as possible while controlling the FDR, defined as $\text{FDR} = \mathbb{E}[(\sum_{j \in \mathcal{D}_{\text{test}}^{\text{null}}} R_j) / \max\{1, \sum_{j \in \mathcal{D}_{\text{test}}} R_j\}]$.

2.2 Review of FDR control with conformal p-values

After randomly partitioning \mathcal{D} into two disjoint subsets $\mathcal{D}_{\text{train}}$ and \mathcal{D}_{cal} , of cardinality n_{train} and $n_{\text{cal}} = n - n_{\text{train}}$ respectively, the standard approach for computing split-conformal p-values begins by training a one-class classification model on the data indexed by $\mathcal{D}_{\text{train}}$. This model is applied out-of-sample to compute conformity scores \hat{S}_i and \hat{S}_j for all calibration and test points $i \in \mathcal{D}_{\text{cal}}$ and $j \in \mathcal{D}_{\text{test}}$, with the convention that larger scores suggest evidence of an outlier. Assuming without loss of generality that all scores take distinct values (otherwise, ties can be broken at random by adding a little noise), a conformal p-value $\hat{u}(X_j)$ for each $j \in \mathcal{D}_{\text{test}}$ is then calculated by taking the relative rank of \hat{S}_j among the \hat{S}_i for all $i \in \mathcal{D}_{\text{cal}}$: $\hat{u}(X_j) = (1 + \sum_{i \in \mathcal{D}_{\text{cal}}} \mathbb{I}\{\hat{S}_j \leq \hat{S}_i\}) / (1 + n_{\text{cal}})$. If the null hypothesis for X_j is true, \hat{S}_j is exchangeable with \hat{S}_i for all $i \in \mathcal{D}_{\text{cal}}$, and $\hat{u}(X_j)$ is uniformly distributed on $\{1/(1 + n_{\text{cal}}), 2/(1 + n_{\text{cal}}), \dots, 1\}$. Since this distribution is stochastically larger than the continuous uniform distribution on $[0, 1]$, one can say that $\hat{u}(X_j)$ is a valid conformal p-value. Note however that the p-values $\hat{u}(X_j)$ and $\hat{u}(X_{j'})$ for two different test points $j, j' \in \mathcal{D}_{\text{test}}$ are not independent of one another, even conditional on $\mathcal{D}_{\text{train}}$, because they share the same calibration data.

Despite their mutual dependence, conformal p-values can be utilized within the BH filter to simultaneously probe the n_{test} hypotheses for all test points while controlling the FDR. A convenient way to explain the BH filter is as follows [34]. Imagine rejecting the null hypothesis for all test points j with $\hat{u}(X_j) \leq s$, for some threshold $s \in [0, 1]$. By monotonicity of $\hat{u}(X_j)$, this amounts to rejecting the null hypothesis for all test points j with $\hat{S}_j \geq t$, for some appropriate threshold $t \in \mathbb{R}$. An intuitive estimate of the proportion of false discoveries incurred by this rule is:

$$\widehat{\text{FDP}}(t) = \frac{n_{\text{test}}}{1 + n_{\text{cal}}} \cdot \frac{1 + \sum_{i \in \mathcal{D}_{\text{cal}}} \mathbb{I}\{\hat{S}_i \geq t\}}{\sum_{j \in \mathcal{D}_{\text{test}}} \mathbb{I}\{\hat{S}_j \geq t\}}. \quad (1)$$

This can be understood by noting that $\sum_{j \in \mathcal{D}_{\text{test}}} \mathbb{I}\{\hat{S}_j^{(k)} \geq t\}$ is the total number of discoveries, while the numerator should behave similarly to the (latent) number of false discoveries in $\mathcal{D}_{\text{test}}$ due to the exchangeability of \hat{S}_i and \hat{S}_j under the null hypothesis. With this notation, it can be shown that the BH filter applied at level $\alpha \in (0, 1)$ computes an adaptive threshold

$$\hat{t}^{\text{BH}} = \min \left\{ t \in \{\hat{S}_i\}_{i \in \mathcal{D}_{\text{cal}} \cup \mathcal{D}_{\text{test}}} : \widehat{\text{FDP}}(t) \leq \alpha \right\}, \quad (2)$$

and rejects all null hypotheses j with $\hat{S}_j \geq \hat{t}^{\text{BH}}$; we refer to Rava et al. [27] for a derivation of this connection. The procedure described above was proved by Bates et al. [9] to control the FDR below α .

2.3 Review of FDR control with AdaDetect

A more sophisticated version of the method reviewed in Section 2.2, called *AdaDetect*, was recently proposed by Marandon et al. [25]. The main difference between the BH procedure applied to conformal p-values and *AdaDetect* is that the latter can leverage a potentially more powerful machine learning model trained by looking also at the calibration samples in \mathcal{D}_{cal} as well as the unlabeled test data in $\mathcal{D}_{\text{test}}$. The only caveat is that the model training process should remain invariant to permutations of the calibration and test samples. While the true inlier or outlier nature of the observations in $\mathcal{D}_{\text{test}}$ is obviously unknown at training time, *AdaDetect* can still extract some useful

information from the test data which would otherwise be ignored by the more traditional split-conformal approach reviewed in Section 2.2. In particular, `AdaDetect` can leverage the test data to automatically tune any desired model hyper-parameters in order to approximately maximize the final number of discoveries. The same idea also motivates the contemporaneous alternative method of *integrative* conformal p-values proposed by Liang et al. [22], although the latter prioritizes testing the null hypothesis for a single test point rather than controlling the FDR and is therefore not discussed in equal detail within this paper. Despite a more sophisticated use of the available data compared to the split-conformal method reviewed in Section 2.2, `AdaDetect` still suffers from the same limitation that it must calibrate its inferences based on a single random data subset \mathcal{D}_{cal} , and thus its results remain aleatory.

For simplicity, in the following we will begin by explaining how to derandomize standard split-conformal inferences; then, the same idea will be easily extended in Section 2.3 to derandomize `AdaDetect`.

3 Method

3.1 Derandomizing split-conformal inferences

Consider $K \geq 1$ repetitions of the split-conformal analysis reviewed in Section 2.2, each starting with an independent split of the reference data into $\mathcal{D}_{\text{train}}^{(k)}$ and $\mathcal{D}_{\text{cal}}^{(k)}$. For each repetition $k \in [K]$, after training the machine learning model on $\mathcal{D}_{\text{train}}^{(k)}$ and computing conformity scores on $\mathcal{D}_{\text{cal}}^{(k)}$ and $\mathcal{D}_{\text{test}}$, one can estimate the false discovery proportion corresponding to the rejection of all test points with scores above a fixed rejection threshold $t \in \mathbb{R}$ as in (1), with:

$$\widehat{\text{FDP}}^{(k)}(t) = \frac{n_{\text{test}}}{1 + n_{\text{cal}}} \cdot \frac{1 + \sum_{i \in \mathcal{D}_{\text{cal}}^{(k)}} \mathbb{I} \left\{ \hat{S}_i^{(k)} \geq t \right\}}{\sum_{j \in \mathcal{D}_{\text{test}}} \mathbb{I} \left\{ \hat{S}_j^{(k)} \geq t \right\}}. \quad (3)$$

Further, for any fixed $\alpha_{\text{bh}} \in (0, 1)$, let $\hat{t}^{(k)}$ be the corresponding BH threshold (2) at the nominal FDR level α_{bh} :

$$\hat{t}^{(k)} = \min \left\{ t \in \tilde{\mathcal{D}}_{\text{cal-test}}^{(k)} : \widehat{\text{FDP}}^{(k)}(t) \leq \alpha_{\text{bh}} \right\}. \quad (4)$$

Then, for each test point $j \in \mathcal{D}_{\text{test}}$, define the following rescaled indicator of whether $\hat{S}_j^{(k)}$ exceeds $\hat{t}^{(k)}$:

$$e_j^{(k)} = (1 + n_{\text{cal}}) \cdot \frac{\mathbb{I} \left\{ \hat{S}_j^{(k)} \geq \hat{t}^{(k)} \right\}}{1 + \sum_{i \in \mathcal{D}_{\text{cal}}^{(k)}} \mathbb{I} \left\{ \hat{S}_i^{(k)} \geq \hat{t}^{(k)} \right\}}. \quad (5)$$

Intuitively, this quantifies not only whether the j -th null hypothesis would be rejected by the BH filter at the nominal FDR level α_{bh} , but also how extreme $\hat{S}_j^{(k)}$ is relative to the calibration scores. This weighting scheme, inspired by Ren and Barber [28], is not the only possible way of derandomizing conformal inferences, but it is carefully designed to achieve valid FDR control as powerfully as possible after aggregating the evidence against the j -th null hypothesis acquired over all K iterations, as explained next. It is worth emphasizing the quantity in (5) follows a slightly relaxed notion of e-value compared to the original definition of Vovk and Wang [38], because it may not always be the case that $\mathbb{E}[e_j^{(k)}] \leq 1$ if X_j is an inlier. Instead, we will show our e-values are valid on average over all test points [28], and that is sufficient for our purposes.

After evaluating (5) for all $j \in \mathcal{D}_{\text{test}}$ and all $k \in [K]$, we aggregate the evidence against the j -th null hypothesis into a single statistic \bar{e}_j by taking a weighted average:

$$\bar{e}_j = \sum_{k=1}^K w^{(k)} e_j^{(k)}, \quad \sum_{k=1}^K w^{(k)} = 1,$$

based on some appropriate normalized weights $w^{(k)}$. Intuitively, the role of $w^{(k)}$ is to allow for the possibility that the machine learning models based on different realizations of the training subset may not all be equally powerful at separating inliers from outliers. In the remainder of this section, we will take these weights to be known a-priori for all $k \in [K]$, thus representing relevant *side information*; e.g., in the sense of Genovese et al. [15] and Ren and Candès [29].

For simplicity, one may think for the time being of a trivial uninformative prior $w^{(k)} = 1/K$. Of course, it would be preferable to allow these weights to be data-driven, but such an extension is deferred to Section 3.2 for conciseness.

Having calculated aggregate e -values \bar{e}_j with the procedure described above, which is outlined by Algorithm A1 in Appendix A1, our method will reject the null hypothesis for all $j \in \mathcal{D}_{\text{test}}$ whose \bar{e}_j is greater than an adaptive threshold calculated by applying the eBH filter of Wang and Ramdas [41], which is outlined for completeness by Algorithm A2 in Appendix A1. We refer to Wang and Ramdas [41] for a more detailed discussion of the eBH filter. Here, it suffices for our purposes to recall that the eBH filter computes an adaptive rejection threshold based on the n_{test} input e -values and on the desired FDR level $\alpha \in (0, 1)$. Then, our following result states that the overall procedure described above is guaranteed to control the FDR below α , under a relatively mild exchangeability assumption.

Assumption 3.1. The inliers in \mathcal{D} and the null test points are exchangeable conditional on the non-null test points.

Theorem 3.2. *Suppose Assumption 3.1 holds. Then, the e -values computed by Algorithm A1 satisfy:*

$$\sum_{j \in \mathcal{D}_{\text{test}}^{\text{null}}} \mathbb{E}[\bar{e}_j] \leq n_{\text{test}}. \quad (6)$$

The proof of Theorem 3.2 is in Appendix A2, along with all other mathematical proofs. Combined with Theorem 2 from Ren and Barber [28], this result implies our method controls the FDR below the desired target level α .

Corollary 3.3 (Ren and Barber [28]). *The eBH filter of Wang and Ramdas [41] applied at level $\alpha \in (0, 1)$ to e -values $\{\bar{e}_j\}_{j \in \mathcal{D}_{\text{test}}}$, satisfying (6) guarantees $\text{FDR} \leq \alpha$.*

Remark 3.4. Assumption 3.1 is a weaker condition compared to assuming the supervised data points and the null test points indexed by $\mathcal{D}_{\text{test}}^{\text{null}}$ are exchangeable with one another and independent of the non-null test points.

Remark 3.5. Theorem 3.2 holds regardless of the value of the hyper-parameter α_{bh} of Algorithm A1, which appears in (4). See Section 3.4 for further details on α_{bh} .

3.2 Leveraging data-driven weights

Our method can be extended to leverage adaptive weights based on the data in \mathcal{D} and $\mathcal{D}_{\text{test}}$, as long as each weight $w^{(k)}$ is invariant to permutations of the test point with the corresponding calibration samples in $\mathcal{D}_{\text{cal}}^{(k)}$. In other words, we only require that these weights be written in the form of

$$w^{(k)} = \omega\left(\tilde{\mathcal{D}}_{\text{cal-test}}^{(k)}\right). \quad (7)$$

Above, the function ω may depend on the data in $\mathcal{D}_{\text{train}}^{(k)}$ but not on $\mathcal{D}_{\text{cal}}^{(k)}$ or $\mathcal{D}_{\text{test}}$. An example of a useful weighting scheme satisfying this property will be provided at the end of this section. The general method is summarized by Algorithm A3 in Appendix A1, which extends Algorithm A1. This produces e -values that control the FDR in conjunction with the eBH filter of Wang and Ramdas [41].

Theorem 3.6. *Suppose Assumption 3.1 holds. Then, the e -values computed by Algorithm A3 satisfy (6), as long as the adaptive weights of Algorithm A3 satisfy (7).*

An example of a valid weighting function applied in this paper is the following. Imagine having some prior side information suggesting that the proportion of outliers in $\mathcal{D}_{\text{test}}$ is approximately $\gamma \in (0, 1)$. Then, a natural choice to measure the quality of the k -th model is to let $\tilde{w}^{(k)} = |\tilde{v}^{(k)}|$, where $\tilde{v}^{(k)}$ is the standard t-statistic for testing the difference in means between the top $\lceil n_{\text{test}} \cdot \gamma \rceil$ largest values in $\tilde{\mathcal{D}}_{\text{cal-test}}^{(k)}$ and the remaining ones. See Algorithm A5 in Appendix A1 for further details. Intuitively, Algorithm A5 tends to assign larger weights to models achieving stronger out-of-sample separation between inliers and outliers. Of course, this approach may not be optimal but different weighting schemes could be easily accommodated within our framework.

3.3 Derandomizing AdaDetect

The requirement discussed in Section 3.2 that the data-adaptive weights should be invariant to permutations of the calibration and test samples is analogous to the idea utilized by AdaDetect [25] to train more powerful machine

learning models leveraging also the information contained in the test set (see Section 2.3). This implies Theorem 3.6 remains valid even if our method is implemented based on K machine learning models each trained by looking also at the unordered union of all data points in $\mathcal{D}_{\text{train}}^{(k)} \cup \mathcal{D}_{\text{test}}$, for each $k \in [K]$. See Algorithm A4 in Appendix A1 for a detailed implementation of this extension of our method, which derandomizes `AdaDetect`.

3.4 Tuning the FDR hyper-parameter

As explained in Section 3.1, our method involves an hyper-parameter α_{bh} controlling the BH thresholds $\hat{t}^{(k)}$ in (4). Intuitively, higher values of α_{bh} tend to increase the number of both test and calibration scores exceeding the rejection threshold at each of the K iterations. Such competing effects make it generally unclear whether increasing α_{bh} leads to larger e-values in (5) and hence higher power. This trade-off was studied by Ren and Barber [28] while derandomizing the knockoff filter, and we follow their suggestion of setting $\alpha_{\text{bh}} = \alpha/2$. This is a reasonable rule of thumb in certain high-power regimes [28], but we leave it to future research to determine whether further improvements are possible. In the meantime, note that a straightforward extension of our method, not explicitly implemented in this paper, can be obtained by further averaging e-values obtained with different choices of α_{bh} . Such extension does not affect the validity of (6) due to the linearity of expected values. Thus, one may say our method can derandomize not only the underlying machine learning model and the split-conformal inference procedure, but also the choice of its own hyper-parameters.

4 Numerical experiments

4.1 Setup and performance metrics

This section compares empirically, on synthetic and real data, the performances of the proposed method, implemented as described in Section 3.3, and that of `AdaDetect`. Both methods are deployed using a binary random forest classifier [25] as the base predictive model. The reason why we focus on derandomizing `AdaDetect` instead of traditional split-conformal inferences based on a one-class classifier [9] is that we observed `AdaDetect` often achieves higher power on the data sets considered in this paper. However, additional experiments reporting on the performance of our method applied with one-class classifiers can be found in Appendix A3.

As the objective of this paper is to powerfully detect outliers while mitigating algorithmic randomness, we assess the performance of each method over $M = 100$ independent analyses based on the same fixed data and the same test set. For each repetition m of the novelty detection analysis based on the fixed data, we identify a subset $\mathcal{R}^{(m)} \subseteq \mathcal{D}_{\text{test}}$ of likely outliers (the rejected null hypotheses) and evaluate the average power and false discovery proportion, namely

$$\widehat{\text{Power}} = \frac{1}{M} \sum_{m=1}^M \frac{|\mathcal{R}^{(m)} \cap \mathcal{D}_{\text{test}}^{\text{non-null}}|}{|\mathcal{D}_{\text{test}}^{\text{non-null}}|}, \quad (8)$$

$$\widehat{\text{FDR}} = \frac{1}{M} \sum_{m=1}^M \frac{|\mathcal{R}^{(m)} \cap \mathcal{D}_{\text{test}}^{\text{null}}|}{\max\{|\mathcal{R}^{(m)}|, 1\}}, \quad (9)$$

where $\mathcal{D}_{\text{test}}^{\text{non-null}} = \mathcal{D}_{\text{test}} \setminus \mathcal{D}_{\text{test}}^{\text{null}}$ indicates the true outliers in the test set. It is worth emphasizing that the average false discovery proportion defined in (9) is not the FDR, which is the quantity we can theoretically guarantee to control. In fact, $\text{FDR} = \mathbb{E}[\widehat{\text{FDR}}]$, with expectation taken with respect all randomness in the data. Nonetheless, we will see that (9) is also controlled in practice within all data sets considered in this paper. The advantage of this setup is that it makes it natural to estimate algorithmic variability by observing the consistency of each rejection across independent analyses. In particular, after defining $R_{j,m}$ as the indicator of whether the j -th null hypothesis was rejected in the m -th analysis, we can evaluate the average variance in the rejection events:

$$\widehat{\text{Variance}} = \frac{1}{n_{\text{test}}} \sum_{j=1}^{n_{\text{test}}} \frac{1}{M-1} \sum_{m=1}^M (R_{j,m} - \bar{R}_j)^2, \quad (10)$$

where $\bar{R}_j = (1/M) \sum_{m=1}^M R_{j,m}$. Intuitively, it would be desirable to have a novelty detection method maximizing power (8) while simultaneously minimizing both the average false discovery proportion (9) and the variability (10).

In practice, however, these metrics often compete with one another; hence why we focus on comparing power and variability for methods designed to control the FDR below the target level $\alpha = 0.1$.

4.2 Experiments with synthetic data

Synthetic reference and test data consisting of 500-dimensional feature vectors X are generated as follows. The reference set contains only inliers, drawn i.i.d. from the standard normal distribution with independent components, $\mathcal{N}(0, I_{500})$. The test set contains 90% inliers and 10% outliers, independently sampled from $\mathcal{N}(\mu, I_{500})$. The first 5 entries of μ are equal to a constant parameter, to which we refer as the *signal amplitude*, while the remaining 495 entries are zeros. The size of the reference set is $n = 1250$, with 750 samples allocated to the training subset and 500 to the calibration subset. The size of the test set is $n_{\text{test}} = 3000$. Both our method and AdaDetect are applied based on the same random forest binary classification classifier, with 100 trees trained to a maximum depth of 10.

4.2.1 The effect of the signal strength

Figure 1 compares the performance of our method (applied with $K = 10$) to that of AdaDetect, as a function of the signal amplitude. The results confirm both methods control the FDR but ours is less variable, as expected. The comparison becomes more interesting when looking at power: AdaDetect tends to detect more outliers on average if the signal strength is low, but our method can also outperform by that metric if the signals are strong. This may be explained as follows. If the signal strength is high, most true discoveries produced by AdaDetect are relatively stable across different analyses, while false discoveries may be more aleatory. Such situation is ideal for derandomization, which explains why our method is able to simultaneously achieve very high power and extremely low false discovery proportion. By contrast, if the signals are weak, the true outlier discoveries produced by AdaDetect are relatively scarce and unpredictable, thus behaving not so differently from the false findings. This makes derandomization arguably even more important from a practical perspective, but unfortunately in this case interpretability and reliability come at the cost of some loss in average power. It is important to emphasize that the notion of algorithmic variability considered in this paper generally tends to be maximized in the medium-power regime, and it naturally goes down to zero when the problem becomes extremely hard, as shown in Figure 1. Nonetheless, it is interesting to note that the inferences output by AdaDetect may remain relatively aleatory even when the power is close to one, while E-AdaDetect overcomes this limitation.

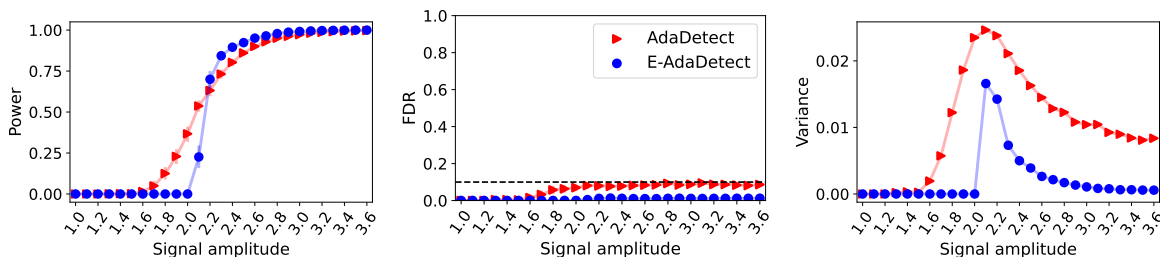


Figure 1: Performance on synthetic data of the proposed derandomized outlier detection method, E-AdaDetect, applied with $K = 10$, compared to that of its randomized benchmark, AdaDetect, as a function of the signal strength. Both methods leverage a random forest binary classifier. Left: average proportion of true outliers that are discovered (higher is better), defined in (8). Center: average proportion of false discoveries (lower is better), defined in (9). Right: variability of the findings (lower is better), as defined in (10).

4.2.2 The effect of the number of analyses K

Figure 2 investigates the effect of varying the number of analyses K aggregated by our method. Here, the signal amplitude is fixed equal to either 2.4 (high-power regime) or 2.1 (low-power regime), while the value of K is varied between 1 and 30. As expected, the results show that the variability of the findings obtained with our method steadily decreases as K increases. Unsurprisingly, the average proportion of false discoveries obtained with our method also tends to decrease as K increases, which can be intuitively understood by noting that spurious findings are less likely to

be reproduced consistently across multiple independent analyses of the same data. Regarding power, the average number of true outliers detected by our method tends to monotonically increase with K if the signal strength is sufficiently high. However, if the signals are weak, our method may start to lose power with larger values of K (although some $K > 1$ may be optimal), consistently with the results in Figure 1. Thus, we recommend practitioners to utilize larger values of K in applications where higher power is expected. Finally, note that the power of our method is generally lower compared to that of *AdaDetect* in the special case of $K = 1$, although this is not a practically relevant value of K because it does not allow any derandomization. The reason why our power is lower if $K = 1$ is that we rely on the eBH filter, which is relatively conservative as an FDR-controlling strategy because it requires no assumptions about the dependency structure of the input statistics.

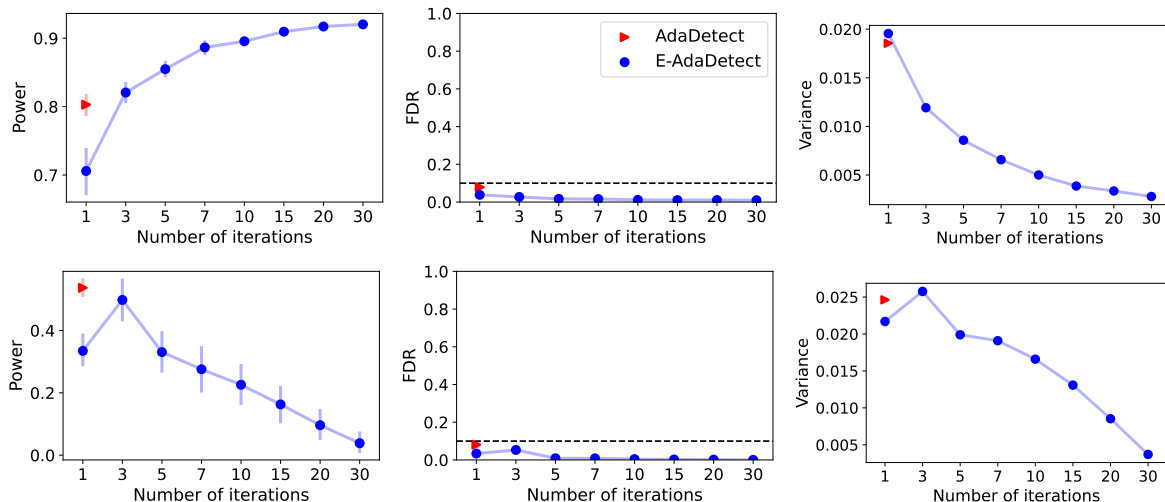


Figure 2: Performance on synthetic data of E-AdaDetect, as a function of the number K of derandomized analyses, compared to its randomized benchmark *AdaDetect*. Note that the latter can only be applied with a single data split (or iteration). Top: high-power regime with signal amplitude 2.4. Bottom: low-power regime with signal amplitude 2.1. Other details are as in Figure 1.

4.2.3 The effect of the weighting strategy

To help highlight the practical advantage of being able to leverage data-adaptive model weights within our method, in this section we carry out experiments similar to those of Figure 1 but leveraging a random forest model trained with slightly different choices of hyper-parameters in each of the K analyses. Specifically, we fit the random forest using $K = 10$ different values of the maximal tree depth, ranging between 1 and 30. Then, we apply our method using different weighting schemes: constant equal weights, data-driven weights calculated with the t-statistic approach summarized in Algorithm A5, and a simple alternative *trimmed average* data-driven approach outlined by Algorithm A6 in Appendix A1. The results show that the data-driven aggregation scheme based on t-statistics is the most effective one, often leading to much higher power. Note that we have chosen not to compare our method to the automatic *AdaDetect* hyper-parameter tuning strategy proposed in Section 4.5 of Marandon et al. [25] because we found that it does not perform very well in our experiments, possibly due to the relatively low sample size.

4.2.4 Additional results

The results of additional experiments with synthetic data are summarized in Appendix A3. Figure A1 confirms the reproducibility of the results in Figure 1 by reporting on the average FDR and power over 100 independent realizations of the data as a function of the signal strength. Figure A2 also reports on experiments similar to those in Figure 1, with the difference that there our method is applied to derandomize classical data splitting instead of *AdaDetect*, and the underlying machine learning model is a one-class support vector classifier instead of a random forest. Figure A3 confirms the reproducibility of the results observed in Figure 2 by reporting on the average FDR and power over

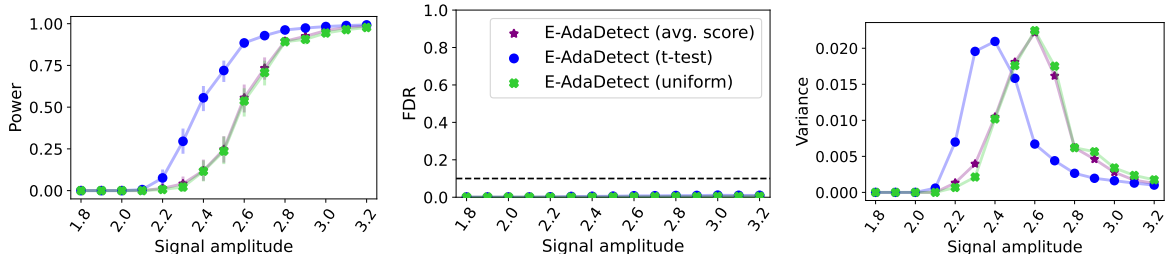


Figure 3: Performance on synthetic data of E-AdaDetect applied with different model weighting schemes, as a function of the signal strength. The model weights are designed to prioritize the results of randomized analyses based on models that are more effective at separating inliers from outliers. The t-test approach tends to lead to higher power. Other details are as in Figure 1.

100 independent realizations of the data as a function of K . Moreover, Figure A4 compares the performances of E-AdaDetect and AdaDetect as a function of the cardinality of the inlier calibration set, having fixed the number of reference inliers in the training set. These results confirm our de-randomization method is effective, and at the same time they also highlight how the power of AdaDetect may decrease as the number of inlier calibration samples increases. Such behaviour may seem surprising at first, because it should not occur with conformal inferences based on one-class classifiers, but it can be understood by recalling that AdaDetect leverages a binary classifier trained under the (incorrect) implicit assumption that all data points in the calibration and test set are outliers. Therefore, it is intuitive that increasing the number of calibration inliers may degrade the power of AdaDetect. Next, Figure A5 compares the performances of E-AdaDetect and AdaDetect as a function of the cardinality of the inlier training set, having fixed the number of inlier calibration samples. Unsurprisingly, the power is now monotone increasing in the number of training inlier data points and similar across AdaDetect and E-AdaDetect, but the latter is much more algorithmically stable. Finally, Figure A6 investigates the performance of E-AdaDetect as a function of its hyper-parameter α_{bh} , showing that values of $\alpha_{bh} \approx \alpha/2$ tend to work relatively well in practice.

4.3 Experiments with real data

We now turn to evaluate the performance of our method on several benchmark data sets for outlier detection, also studied in Bates et al. [9] and Marandon et al. [25]: *mammography* [3], *musk* [4], *shuttle* [5], *KDDCup99* [1], and *credit card* [2]. We refer to Bates et al. [9] and Marandon et al. [25] for more details about these data sets. Similarly to Section 4.2, we construct a reference set and a test set through random sub-sampling. The reference set contains 3000 inliers, and the test set contains 1000 samples, of which 10% are outliers. Our method is applied to derandomize AdaDetect over $K = 10$ independent splits of the reference set into training and calibration subsets of size 2000 and 1000, respectively. Both our method and AdaDetect are repeatedly applied to carry out 100 independent analyses of the same data. The results, summarized in Figure 4, demonstrate both methods control the average proportion of false discoveries below $\alpha = 0.1$ and achieve similar power, but the findings obtained with our method are far more stable. Finally, Figure A7 in Appendix A4 confirms the reproducibility of these results by reporting the average FDR and power over 100 independent realizations of the sub-sampled data considered in Figure 4.

5 Discussion

Our experience suggests that e-values are often less powerful than p-values in measuring the statistical evidence against a *single hypothesis*. Yet, e-values can be useful to aggregate multiple dependent tests of the same hypothesis [38]—a task that would otherwise require very conservative adjustments within the p-value framework [40]. Further, e-values lend themselves very well to *multiple testing* because they allow efficient FDR control under arbitrary dependence [41], and even their relatively weak *individual* evidence can accumulate rapidly when a large number of hypotheses is probed. The opportunity arising from the combination of these two key properties was recently leveraged to derandomize knockoffs [28], but until now it had not been fully exploited in conformal inference.

While this paper has focused on derandomizing split-conformal inferences for novelty detection, the key ideas

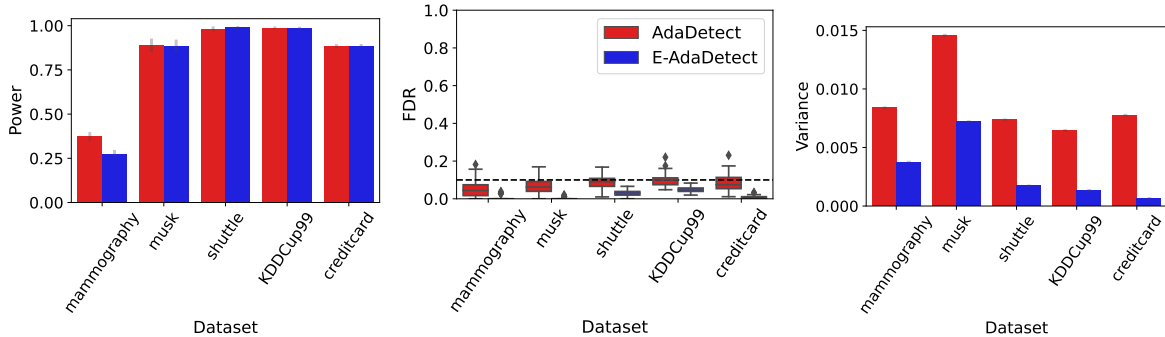


Figure 4: Performance on real data of *AdaDetect* and its randomized version, *E-AdaDetect*. Both methods leverage a random forest binary classifier. Left: average proportion of true outliers that are discovered (higher is better). Center: average proportion of false discoveries (lower is better). Right: variability of the findings (lower is better).

could be easily extended. For example, one may utilize e-values to derandomize conformal prediction intervals in regression [20, 31] or conformal prediction sets in multi-class classification [21, 32] while controlling the false coverage rate over a large test set [42]. A different direction for future research may explore the derandomization of alternative methods such as cross-validation+ [8]. The latter is already intrinsically more stable compared to split-conformal inference, but it can still be affected by other sources of algorithmic variability including randomized model initialization and arbitrary hyper-parameter tuning. Moreover, cross-validation+ p-values require a conservative theoretical correction [8] that appears often unnecessary in practice, and they are mutually dependent in a way that complicates FDR control. Therefore, it seems worth exploring the combination of e-value and cross-validation+ ideas in the context of FDR or false coverage rate control.

We conclude by emphasizing two limitations of this work. First, the proposed method is more computationally expensive compared to standard split-conformal inference or *AdaDetect*, and therefore one may be limited to applying it with relatively small numbers K of analysis repetitions when working with extremely large data sets. Yet, this may not be a crucial limitation because it is increasingly recognized that stability, reproducibility, and interpretability are sufficiently important goals in data science to often justify the deployment of additional resources [45, 44]. Second, the numerical experiments presented in this paper have shown that our method sometimes leads to a reduction in the average number of findings compared to randomized alternatives, especially in applications where few discoveries are expected. Therefore, in situations with few anticipated discoveries, practitioners considering to apply our method should carefully weight the obvious gains in interpretability versus a possible reduction in power.

Software implementing the algorithms described in this paper and enabling the reproduction of the associated numerical experiments is available at <https://github.com/Meshiba/derandomized-novelty-detection>.

Acknowledgements

Y. R. and M. B. were supported by the Israel Science Foundation (grant No. 729/21). Y. R. thanks the Career Advancement Fellowship, Technion, for providing research support. Y. R. also thanks Citi for the generous financial support. M. S. is partially supported by the National Science Foundation (grant DMS 2210637) and by an Amazon Research Award.

References

- [1] KDD Cup 1999 Data Set. <https://www.kaggle.com/mlg-ulb/creditcardfraud>. Not normalized, without duplicates, categorical attributes removed. Accessed: January, 2021.
- [2] Credit Card Fraud Detection Data Set. <https://www.kaggle.com/mlg-ulb/creditcardfraud>. Accessed: January, 2021.

- [3] Mammography Data Set. <http://odds.cs.stonybrook.edu/mammography-dataset/>. Accessed: January, 2021.
- [4] Statlog (Musk) Data Set. <http://odds.cs.stonybrook.edu/musk-dataset>. Accessed: January, 2021.
- [5] Statlog (Shuttle) Data Set. <http://odds.cs.stonybrook.edu/shuttle-dataset>. Accessed: January, 2021.
- [6] M. Ahmed, A. N. Mahmood, and M. R. Islam. A survey of anomaly detection techniques in financial domain. *Future Generation Computer Systems*, 55:278–288, 2016.
- [7] R. F. Barber and E. Candès. Controlling the false discovery rate via knockoffs. *Annals of Statistics*, 43(5): 2055–2085, 2015.
- [8] R. F. Barber, E. Candès, A. Ramdas, R. J. Tibshirani, et al. Predictive inference with the jackknife+. *Annals of Statistics*, 49(1):486–507, 2021.
- [9] S. Bates, E. Candès, L. Lei, Y. Romano, and M. Sesia. Testing for outliers with conformal p-values. *arXiv preprint arXiv:2104.08279*, 2021.
- [10] D. Beganovic and E. Smirnov. Ensemble cross-conformal prediction. In *2018 IEEE International Conference on Data Mining Workshops*, pages 870–877. IEEE, 2018.
- [11] Y. Benjamini and Y. Hochberg. Controlling the false discovery rate: a practical and powerful approach to multiple testing. *Journal of the Royal statistical society: series B (Methodological)*, 57(1):289–300, 1995.
- [12] Y. Benjamini and D. Yekutieli. The control of the false discovery rate in multiple testing under dependency. *Annals of statistics*, pages 1165–1188, 2001.
- [13] V. Chandola, A. Banerjee, and V. Kumar. Anomaly detection: A survey. *ACM computing surveys (CSUR)*, 41(3): 1–58, 2009.
- [14] W. Fithian and L. Lei. Conditional calibration for false discovery rate control under dependence. *Annals of Statistics*, 50(6):3091–3118, 2022.
- [15] C. R. Genovese, K. Roeder, and L. Wasserman. False discovery control with p-value weighting. *Biometrika*, 93(3):509–524, 2006.
- [16] L. Guan and R. Tibshirani. Prediction and outlier detection in classification problems. *arXiv preprint arXiv:1905.04396*, 2019.
- [17] C. Gupta, A. K. Kuchibhotla, and A. Ramdas. Nested conformal prediction and quantile out-of-bag ensemble methods. *Pattern Recognition*, 127:108496, 2022.
- [18] B. Kim, C. Xu, and R. Barber. Predictive inference is free with the jackknife+-after-bootstrap. *Adv. Neural Inf. Process. Syst.*, 33:4138–4149, 2020.
- [19] R. Laxhammar and G. Falkman. Inductive conformal anomaly detection for sequential detection of anomalous sub-trajectories. *Annals of Mathematics and Artificial Intelligence*, 74(1-2):67–94, 2015.
- [20] J. Lei and L. Wasserman. Distribution-free prediction bands for non-parametric regression. *Journal of the Royal Statistical Society: Series B (Statistical Methodology)*, 76(1):71–96, 2014. doi: 10.1111/rssb.12021.
- [21] J. Lei, J. Robins, and L. Wasserman. Distribution-free prediction sets. *Journal of the American Statistical Association*, 108(501):278–287, 2013. doi: 10.1080/01621459.2012.751873.
- [22] Z. Liang, M. Sesia, and W. Sun. Integrative conformal p-values for powerful out-of-distribution testing with labeled outliers. *arXiv preprint arXiv:2208.11111*, 2022.
- [23] H. Linusson, U. Johansson, and H. Boström. Efficient conformal predictor ensembles. *Neurocomputing*, 397: 266–278, 2020.

- [24] T. Löfström, U. Johansson, and H. Boström. Effective utilization of data in inductive conformal prediction. In *Proc. Int. Jt. Conf. Neural Netw.* IEEE, 2013.
- [25] A. Marandon, L. Lei, D. Mary, and E. Roquain. Machine learning meets false discovery rate. *arXiv preprint arXiv:2208.06685*, 2022.
- [26] M. M. Moya, M. W. Koch, and L. D. Hostetler. One-class classifier networks for target recognition applications. *NASA STI/Recon Technical Report N*, 93:24043, 1993.
- [27] B. Rava, W. Sun, G. M. James, and X. Tong. A burden shared is a burden halved: A fairness-adjusted approach to classification. *arXiv preprint arXiv:2110.05720*, 2021.
- [28] Z. Ren and R. F. Barber. Derandomized knockoffs: leveraging e-values for false discovery rate control. *arXiv preprint arXiv:2205.15461*, 2022.
- [29] Z. Ren and E. Candès. Knockoffs with side information. *arXiv preprint arXiv:2001.07835*, 2020.
- [30] M. Riani, A. C. Atkinson, and A. Cerioli. Finding an unknown number of multivariate outliers. *Journal of the Royal Statistical Society: series B (statistical methodology)*, 71(2):447–466, 2009.
- [31] Y. Romano, E. Patterson, and E. Candès. Conformalized quantile regression. In *Advances in Neural Information Processing Systems 32*, pages 3543–3553. 2019.
- [32] Y. Romano, M. Sesia, and E. Candès. Classification with valid and adaptive coverage. *Advances in Neural Information Processing Systems*, 33, 2020.
- [33] J. Smith, I. Nouretdinov, R. Craddock, C. Offer, and A. Gammerman. Conformal anomaly detection of trajectories with a multi-class hierarchy. In *International symposium on statistical learning and data sciences*, pages 281–290. Springer, 2015.
- [34] J. D. Storey. A direct approach to false discovery rates. *Journal of the Royal Statistical Society: Series B (Statistical Methodology)*, 64(3):479–498, 2002.
- [35] L. Tarassenko, P. Hayton, N. Cerneaz, and M. Brady. Novelty detection for the identification of masses in mammograms. In *1995 Fourth International Conference on Artificial Neural Networks*, pages 442–447. IET, 1995.
- [36] V. Vovk. Transductive conformal predictors. In *IFIP International Conference on Artificial Intelligence Applications and Innovations*, pages 348–360. Springer, 2013.
- [37] V. Vovk and R. Wang. Combining p-values via averaging. *Biometrika*, 107(4):791–808, 2020.
- [38] V. Vovk and R. Wang. E-values: Calibration, combination and applications. *Annals of Statistics*, 49(3), jun 2021.
- [39] V. Vovk, A. Gammerman, and G. Shafer. *Algorithmic learning in a random world*. Springer, 2005.
- [40] V. Vovk, B. Wang, and R. Wang. Admissible ways of merging p-values under arbitrary dependence. *Annals of Statistics*, 50(1):351–375, 2022.
- [41] R. Wang and A. Ramdas. False discovery rate control with e-values. *arXiv preprint arXiv:2009.02824*, 2020.
- [42] A. Weinstein and A. Ramdas. Online control of the false coverage rate and false sign rate. In *International Conference on Machine Learning*, pages 10193–10202. PMLR, 2020.
- [43] S. S. Wilks. Multivariate statistical outliers. *Sankhyā: The Indian Journal of Statistics, Series A*, pages 407–426, 1963.
- [44] B. Yu. Stability expanded, in reality. *Harvard Data Science Review*, 2020.
- [45] B. Yu and K. Kumbier. Veridical data science. *Proceedings of the National Academy of Sciences*, 117(8): 3920–3929, 2020.
- [46] M. Zhang, A. Raghunathan, and N. K. Jha. MedMon: Securing medical devices through wireless monitoring and anomaly detection. *IEEE Transactions on Biomedical Circuits and Systems*, 7(6):871–881, 2013.

A1 Algorithmic details

Algorithm A1 Aggregation of conformal e-values with fixed model weights

- 1: **Input:** inlier data set $\mathcal{D} \equiv \{X_i\}_{i=1}^n$; test set $\mathcal{D}_{\text{test}}$; size of calibration-set n_{cal} ; number of iterations K ; one-class or binary black-box classification algorithm \mathcal{A} ; normalized model weights $w^{(k)}$, for $k \in [K]$; hyper-parameter $\alpha_{\text{bh}} \in (0, 1)$;
 - 2: **for** $k = 1, \dots, K$ **do**
 - 3: Randomly split \mathcal{D} into $\mathcal{D}_{\text{cal}}^{(k)}$ and $\mathcal{D}_{\text{train}}^{(k)}$, with $|\mathcal{D}_{\text{cal}}^{(k)}| = n_{\text{cal}}$
 - 4: Train the model: $\mathcal{M}^{(k)} \leftarrow \mathcal{A}(\mathcal{D}_{\text{train}}^{(k)})$ {possibly including additional labeled outlier data if available}
 - 5: Compute the calibration scores $S_i^{(k)} = \mathcal{M}^{(k)}(X_i)$, for all $i \in \mathcal{D}_{\text{cal}}^{(k)}$
 - 6: Compute the test scores $S_j^{(k)} = \mathcal{M}^{(k)}(X_j)$, for all $j \in \mathcal{D}_{\text{test}}$
 - 7: Compute the threshold $\hat{t}^{(k)}$ according to (4) {this depends on the hyper-parameter α_{bh} }
 - 8: Compute the e-values $e_j^{(k)}$ for all $j \in |\mathcal{D}_{\text{test}}|$ according to (5)
 - 9: **end for**
 - 10: Aggregate the e-values $\bar{e}_j = \sum_{k=1}^K w^{(k)} \cdot e_j^{(k)}$
 - 11: **Output:** e-values \bar{e}_j for all $j \in \mathcal{D}_{\text{test}}$ that can be filtered with Algorithm A2 to control the FDR.
-

Algorithm A2 eBH filter of Wang and Ramdas [41]

- 1: **Input:** e-values $\{e_j\}_{j=1}^N$ corresponding to N null hypotheses to be tested; target FDR level $\alpha \in (0, 1)$
 - 2: Compute the order statistics of the e-values: $e_{(1)} \geq \dots \geq e_{(N)}$
 - 3: Find the rejection threshold $i_{\text{max}} = \max\{i \in [N] : e_{(i)} \geq N/(\alpha \cdot i)\}$
 - 4: Construct the rejection set $\mathcal{R} = \{j \in [N] : e_j \geq e_{(i_{\text{max}})}\}$
 - 5: **Output:** a list of rejected null hypotheses $\mathcal{R} \subseteq [N]$.
-

Algorithm A3 Aggregation of conformal e-values with data-adaptive model weights

- 1: **Input:** inlier data set $\mathcal{D} \equiv \{X_i\}_{i=1}^n$; test set $\mathcal{D}_{\text{test}}$; size of calibration-set n_{cal} ; number of iterations K ; one-class or binary black-box classification algorithm \mathcal{A} ; a model weighting function ω ; hyper-parameter $\alpha_{\text{bh}} \in (0, 1)$;
 - 2: **for** $k = 1, \dots, K$ **do**
 - 3: Randomly split \mathcal{D} into $\mathcal{D}_{\text{cal}}^{(k)}$ and $\mathcal{D}_{\text{train}}^{(k)}$, with $|\mathcal{D}_{\text{cal}}^{(k)}| = n_{\text{cal}}$
 - 4: Train the model: $\mathcal{M}^{(k)} \leftarrow \mathcal{A}(\mathcal{D}_{\text{train}}^{(k)})$ {possibly including additional labeled outlier data if available}
 - 5: Compute the calibration scores $S_i^{(k)} = \mathcal{M}^{(k)}(X_i)$, for all $i \in \mathcal{D}_{\text{cal}}^{(k)}$
 - 6: Compute the test scores $S_j^{(k)} = \mathcal{M}^{(k)}(X_j)$, for all $j \in \mathcal{D}_{\text{test}}$
 - 7: Compute the weights $\tilde{w}^{(k)} = \omega\left(\{S_i\}_{i \in \mathcal{D}_{\text{test}} \cup \mathcal{D}_{\text{cal}}^{(k)}}\right)$ {invariant un-normalized model weights}
 - 8: Compute the threshold $\hat{t}^{(k)}$ according to (4) {this depends on the hyper-parameter α_{bh} }
 - 9: Compute the e-values $e_j^{(k)}$ for all $j \in |\mathcal{D}_{\text{test}}|$ according to (5)
 - 10: **end for**
 - 11: **for** $k = 1, \dots, K$ **do**
 - 12: $w^{(k)} = \tilde{w}^{(k)} / \sum_{k'=1}^K \tilde{w}^{(k')}$ {normalize the model weights}
 - 13: **end for**
 - 14: Aggregate the e-values $\bar{e}_j = \sum_{k=1}^K w^{(k)} \cdot e_j^{(k)}$
 - 15: **Output:** e-values \bar{e}_j for all $j \in \mathcal{D}_{\text{test}}$ that can be filtered with Algorithm A2 to control the FDR.
-

Algorithm A4 Aggregation of conformal e-values with data-adaptive model weights and AdaDetect training

- 1: **Input:** inlier data set $\mathcal{D} \equiv \{X_i\}_{i=1}^n$; test set $\mathcal{D}_{\text{test}}$; size of calibration-set n_{cal} ; number of iterations K ; black-box binary classification algorithm \mathcal{A} ; a model weighting function ω ; hyper-parameter $\alpha_{\text{bh}} \in (0, 1)$;
 - 2: **for** $k = 1, \dots, K$ **do**
 - 3: Randomly split \mathcal{D} into $\mathcal{D}_{\text{cal}}^{(k)}$ and $\mathcal{D}_{\text{train}}^{(k)}$, with $|\mathcal{D}_{\text{cal}}^{(k)}| = n_{\text{cal}}$
 - 4: Train the binary classifier, $\mathcal{M}^{(k)} \leftarrow \mathcal{A}(\mathcal{D}_{\text{train}}^{(k)}, \mathcal{D}_{\text{cal}}^{(k)} \cup \mathcal{D}_{\text{test}})$ {treating the data in $\mathcal{D}_{\text{cal}}^{(k)} \cup \mathcal{D}_{\text{test}}$ as outliers}
 - 5: Compute the calibration scores $S_i^{(k)} = \mathcal{M}^{(k)}(X_i)$, for all $i \in \mathcal{D}_{\text{cal}}^{(k)}$
 - 6: Compute the test scores $S_j^{(k)} = \mathcal{M}^{(k)}(X_j)$, for all $j \in \mathcal{D}_{\text{test}}$
 - 7: Compute the weights $\tilde{w}^{(k)} = \omega\left(\{S_i\}_{i \in \mathcal{D}_{\text{test}} \cup \mathcal{D}_{\text{cal}}^{(k)}}\right)$ {invariant un-normalized model weights}
 - 8: Compute the threshold $\hat{t}^{(k)}$ according to (4) {this depends on the hyper-parameter α_{bh} }
 - 9: Compute the e-values $e_j^{(k)}$ for all $j \in |\mathcal{D}_{\text{test}}|$ according to (5)
 - 10: **end for**
 - 11: **for** $k = 1, \dots, K$ **do**
 - 12: $w^{(k)} = \tilde{w}^{(k)} / \sum_{k'=1}^K \tilde{w}^{(k')}$ {normalize the model weights}
 - 13: **end for**
 - 14: Aggregate the e-values $\bar{e}_j = \sum_{k=1}^K w^{(k)} \cdot e_j^{(k)}$
 - 15: **Output:** e-values \bar{e}_j for all $j \in \mathcal{D}_{\text{test}}$ that can be filtered with Algorithm A2 to control the FDR.
-

Algorithm A5 Adaptive model weighting via t-tests

- 1: **Input:** Scores $\{S_i\}_{i=1}^N$; a guess γ for the proportion of outliers in the data.
 - 2: Compute the order statistics of the scores: $S_{(1)} \leq \dots \leq S_{(N)}$
 - 3: Denote $n_2 = \lceil \gamma N \rceil$ and $n_1 = N - n_2$
 - 4: Divide the sorted scores into two groups with size n_1 and n_2 : $\mathcal{I}_1 = \{S_{(i)}\}_{i=1}^{n_1}$, $\mathcal{I}_2 = \{S_{(i)}\}_{i=n_1+1}^N$
 - 5: Estimate the means of the two groups: $\mu_1 = (1/n_1) \sum_{i \in \mathcal{I}_1} S_{(i)}$ and $\mu_2 = (1/n_2) \sum_{i \in \mathcal{I}_2} S_{(i)}$
 - 6: Estimate the pooled variance: $z = (1/(n_1 + n_2 - 2)) [\sum_{i \in \mathcal{I}_1} (S_{(i)} - \mu_1)^2 + \sum_{i \in \mathcal{I}_2} (S_{(i)} - \mu_2)^2]$
 - 7: Compute the t-statistic: $\tilde{v} = (\mu_1 - \mu_2) / \sqrt{z \cdot (1/n_1 + 1/n_2)}$
 - 8: **Output:** model weight $\tilde{w} = |\tilde{v}|$
-

Algorithm A6 Adaptive model weighting via trimmed mean

- 1: **Input:** Scores $\{S_i\}_{i=1}^N$; a guess γ for the proportion of outliers in the data.
 - 2: Compute the order statistics of the scores: $S_{(1)} \leq \dots \leq S_{(N)}$
 - 3: Denote $\tilde{n} = N - \lceil \gamma N \rceil$
 - 4: Compute the mean of the trimmed group: $\hat{\mu} = \sum_{i=1}^{\tilde{n}} S_{(i)}$
 - 5: **Output:** model weight $\tilde{w} = e^{-\hat{\mu}}$
-

A2 Mathematical proofs

Proof of Theorem 3.2. This result is implied by Theorem 3.6, to whose proof we refer. \square

Proof of Theorem 3.6. The proof follows a martingale argument similar to that of Rava et al. [27]. For each fixed k , define the following two quantities as functions of $t \in \mathbb{R}$:

$$V_{\text{test}}^{(k)}(t) = \sum_{j \in \mathcal{D}_{\text{test}}^{\text{null}}} \mathbb{I} \left\{ S_j^{(k)} \geq \hat{t}^{(k)} \right\}, \quad (\text{A11})$$

and

$$V_{\text{cal}}^{(k)}(t) = \sum_{i \in \mathcal{D}_{\text{cal}}^{(k)}} \mathbb{I} \left\{ S_i^{(k)} \geq \hat{t}^{(k)} \right\}. \quad (\text{A12})$$

For each iteration $k \in [K]$, define also the unordered set of conformity scores for non-null test points as:

$$\tilde{\mathcal{D}}_{\text{test-nn}}^{(k)} = \{\hat{S}_i^{(k)}\}_{i \in \mathcal{D}_{\text{test}} \setminus \mathcal{D}_{\text{test}}^{\text{null}}},$$

and the unordered set of conformity scores for all calibration and test points as:

$$\tilde{\mathcal{D}}_{\text{cal-test}}^{(k)} = \{\hat{S}_i^{(k)}\}_{i \in \mathcal{D}_{\text{test}} \cup \mathcal{D}_{\text{cal}}^{(k)}}.$$

With this premise, we can write:

$$\begin{aligned} \sum_{j \in \mathcal{D}_{\text{test}}^{\text{null}}} \mathbb{E} [\bar{e}_j] &= \sum_{j \in \mathcal{D}_{\text{test}}^{\text{null}}} \mathbb{E} \left[\sum_{k=1}^K w^{(k)} e_j^{(k)} \right] \\ &= \sum_{k=1}^K \sum_{j \in \mathcal{D}_{\text{test}}^{\text{null}}} \mathbb{E} \left[w^{(k)} e_j^{(k)} \right] \\ &= \sum_{k=1}^K \sum_{j \in \mathcal{D}_{\text{test}}^{\text{null}}} \mathbb{E} \left[w^{(k)} (1 + n_{\text{cal}}) \frac{\mathbb{I} \left\{ S_j^{(k)} \geq \hat{t}^{(k)} \right\}}{1 + V_{\text{cal}}^{(k)}(\hat{t}^{(k)})} \right] \\ &= \sum_{k=1}^K \mathbb{E} \left[w^{(k)} (1 + n_{\text{cal}}) \mathbb{E} \left[\frac{V_{\text{test}}^{(k)}(\hat{t}^{(k)})}{1 + V_{\text{cal}}^{(k)}(\hat{t}^{(k)})} \mid \tilde{\mathcal{D}}_{\text{cal-test}}^{(k)}, \tilde{\mathcal{D}}_{\text{test-nn}}^{(k)} \right] \right] \\ &= \sum_{k=1}^K \mathbb{E} \left[w^{(k)} \cdot n_{\text{test}}^{\text{null}} \right] \\ &= n_{\text{test}}^{\text{null}} \leq n_{\text{test}}. \end{aligned}$$

Above, the third-to-last equality follows from the assumption that $w^{(k)}$ is a deterministic function of $\tilde{\mathcal{D}}_{\text{cal-test}}^{(k)}$, and the second-to-last equality follows from the fact that $M^{(k)}(t)$, defined as

$$M^{(k)}(t) = \frac{V_{\text{test}}^{(k)}(t)}{1 + V_{\text{cal}}^{(k)}(t)},$$

is a martingale conditional on $\tilde{\mathcal{D}}_{\text{cal-test}}^{(k)}$ and $\tilde{\mathcal{D}}_{\text{test-nn}}^{(k)}$, and therefore

$$\mathbb{E} \left[M^{(k)}(\hat{t}^{(k)}) \mid \tilde{\mathcal{D}}_{\text{cal-test}}^{(k)}, \tilde{\mathcal{D}}_{\text{test-nn}}^{(k)} \right] = \frac{n_{\text{test}}^{\text{null}}}{1 + n_{\text{cal}}}.$$

This last statement is proved below, following the same strategy as in Rava et al. [27].

For each $l \in \{1, \dots, n_{\text{test}} + n_{\text{cal}}\}$, define t_l as the smallest threshold t at which exactly l outliers have scores exceeding t , across all calibration and null test points:

$$t_l^{(k)} = \inf \left\{ t : V_{\text{test}}^{(k)}(t) + V_{\text{cal}}^{(k)}(t) \geq l \right\}.$$

By convention, we also define $t_0^{(k)} = -\infty$. Consider then the following discrete-time filtration indexed by l :

$$\mathcal{F}_l^{(k)} = \left\{ \sigma \left(V_{\text{test}}^{(k)}(t_{l'}^{(k)}), V_{\text{cal}}^{(k)}(t_{l'}^{(k)}) \right) \right\}_{0 \leq l' \leq l}.$$

For any $l \in \{1, \dots, n_{\text{test}} + n_{\text{cal}}\}$, it follows from Assumption 3.1 that

$$\begin{aligned} & \mathbb{E} \left[M^{(k)}(t_{l-1}^{(k)}) \mid \mathcal{F}_l^{(k)}, \tilde{\mathcal{D}}_{\text{cal-test}}^{(k)}, \tilde{\mathcal{D}}_{\text{test-nn}}^{(k)} \right] \\ &= \frac{V_{\text{test}}^{(k)}(t_{l-1}^{(k)})}{V_{\text{cal}}^{(k)}(t_{l-1}^{(k)})} \cdot \frac{V_{\text{cal}}^{(k)}(t_{l-1}^{(k)})}{V_{\text{cal}}^{(k)}(t_{l-1}^{(k)}) + V_{\text{test}}^{(k)}(t_{l-1}^{(k)})} + \frac{V_{\text{test}}^{(k)}(t_{l-1}^{(k)}) - 1}{1 + V_{\text{cal}}^{(k)}(t_{l-1}^{(k)})} \cdot \frac{V_{\text{test}}^{(k)}(t_{l-1}^{(k)})}{V_{\text{cal}}^{(k)}(t_{l-1}^{(k)}) + V_{\text{test}}^{(k)}(t_{l-1}^{(k)})} \\ &= \frac{V_{\text{test}}^{(k)}(t_{l-1}^{(k)})}{V_{\text{cal}}^{(k)}(t_{l-1}^{(k)}) + V_{\text{test}}^{(k)}(t_{l-1}^{(k)})} + \frac{V_{\text{test}}^{(k)}(t_{l-1}^{(k)}) - 1}{1 + V_{\text{cal}}^{(k)}(t_{l-1}^{(k)})} \cdot \frac{V_{\text{test}}^{(k)}(t_{l-1}^{(k)})}{V_{\text{cal}}^{(k)}(t_{l-1}^{(k)}) + V_{\text{test}}^{(k)}(t_{l-1}^{(k)})} \\ &= \frac{V_{\text{test}}^{(k)}(t_{l-1}^{(k)}) \cdot [1 + V_{\text{cal}}^{(k)}(t_{l-1}^{(k)})] + V_{\text{test}}^{(k)}(t_{l-1}^{(k)}) \cdot [V_{\text{test}}^{(k)}(t_{l-1}^{(k)}) - 1]}{[1 + V_{\text{cal}}^{(k)}(t_{l-1}^{(k)})] \cdot [V_{\text{cal}}^{(k)}(t_{l-1}^{(k)}) + V_{\text{test}}^{(k)}(t_{l-1}^{(k)})]} \\ &= \frac{V_{\text{test}}^{(k)}(t_{l-1}^{(k)})}{1 + V_{\text{cal}}^{(k)}(t_{l-1}^{(k)})} \\ &= M^{(k)}(t_l^{(k)}). \end{aligned}$$

By the optional stopping theorem, this implies that

$$\mathbb{E} \left[M^{(k)}(\hat{t}^{(k)}) \mid \tilde{\mathcal{D}}_{\text{cal-test}}^{(k)}, \tilde{\mathcal{D}}_{\text{test-nn}}^{(k)} \right] = \mathbb{E} \left[M^{(k)}(t_0) \mid \tilde{\mathcal{D}}_{\text{cal-test}}^{(k)}, \tilde{\mathcal{D}}_{\text{test-nn}}^{(k)} \right] = \frac{n_{\text{test}}^{\text{null}}}{1 + n_{\text{cal}}},$$

and this completes the proof. □

A3 Additional results from experiments with synthetic data

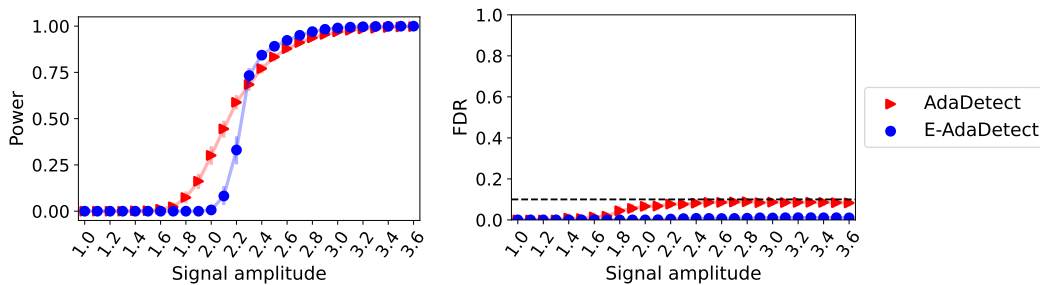


Figure A1: Performance on synthetic data of the proposed derandomized outlier detection method, E-AdaDetect, applied with $K = 10$, compared to that of its randomized benchmark, AdaDetect, as a function of the signal strength. The results are averaged over 100 independent realizations of the data. Left: average proportion of true outliers that are discovered (higher is better). Right: average proportion of false discoveries (lower is better). Other results are as in Figure 1.

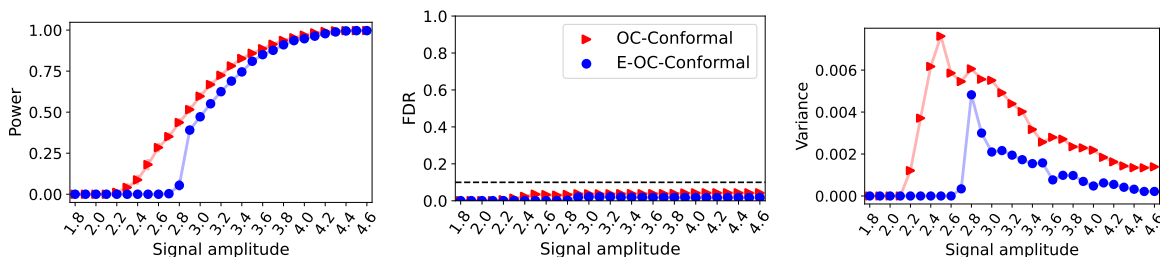


Figure A2: Performance on synthetic data of the proposed derandomized outlier detection method, E-OC-Conformal, applied with $K = 10$, compared to that of its randomized benchmark, OC-Conformal, as a function of the signal strength. Both methods leverage a one-class support vector classifier. Left: average proportion of true outliers that are discovered (higher is better). Center: average proportion of false discoveries (lower is better). Right: variability of the findings (lower is better). The synthetic data here are 100-dimensional. The E-OC-Conformal method is applied with two different values of the α_{bh} hyper-parameter, $\alpha_{bh} = 0.05$ and $\alpha_{bh} = 0.07$, and the results are then aggregated as explained in Section 3.4. Other details are as in Figure 1.

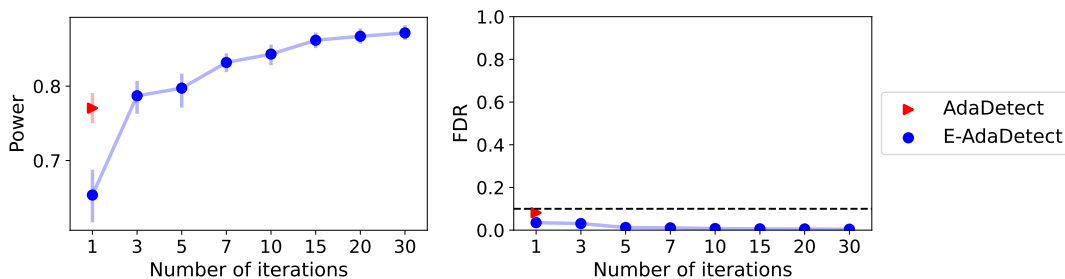


Figure A3: Performance on synthetic data of E-AdaDetect, as a function of the number K of derandomized analyses, compared to that of its randomized benchmark AdaDetect. The results are averaged over 100 independent realizations of the data. The signal amplitude is 2.4 (high-power regime). Left: average proportion of true outliers that are discovered (higher is better). Right: average proportion of false discoveries (lower is better). Other results are as in Figure 2.

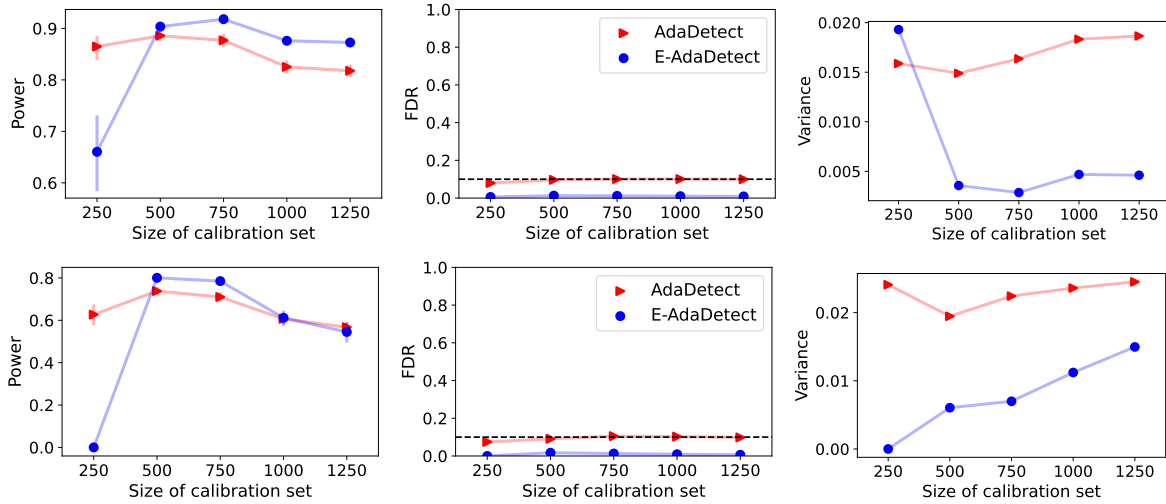


Figure A4: Performance on synthetic data of the proposed derandomized outlier detection method, E-AdaDetect, applied with $K = 10$, compared to that of its randomized benchmark, AdaDetect, as a function of the number of inlier calibration points. The number of training inliers is fixed to 1000. Top: high-power regime with signal amplitude 2.4. Bottom: low-power regime with signal amplitude 2.1. Other details are as in Figure 1. Note that these results correspond to 100 repeated experiments based on a single realization of the labeled and test data, hence why the results appear a little noisy.

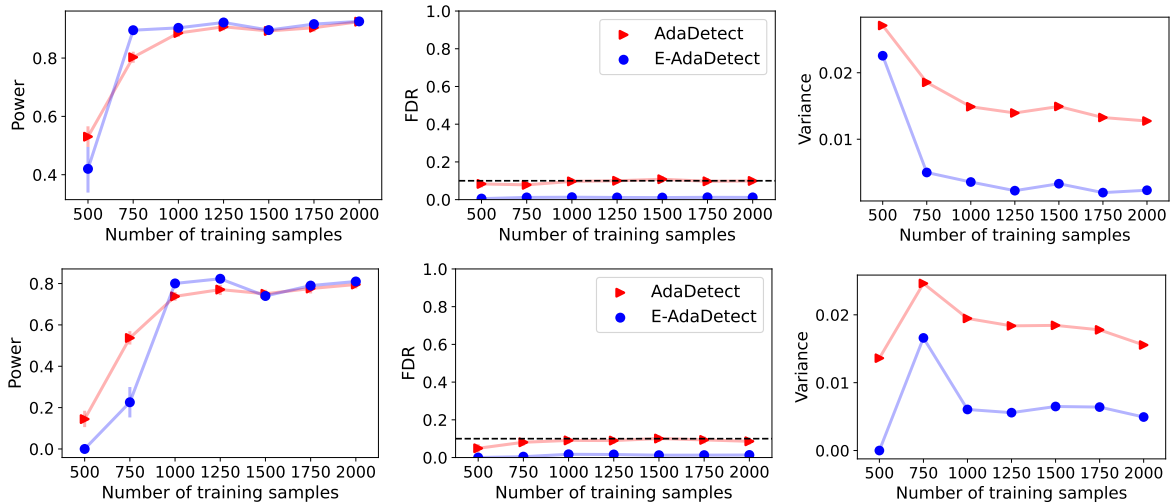


Figure A5: Performance on synthetic data of the proposed derandomized outlier detection method, E-AdaDetect, applied with $K = 10$, compared to that of its randomized benchmark, AdaDetect, as a function of the number of inlier training points. The number of inlier calibration data points is fixed to 500. Note that these results correspond to 100 repeated experiments based on a single realization of the labeled and test data, hence why the results appear a little noisy.

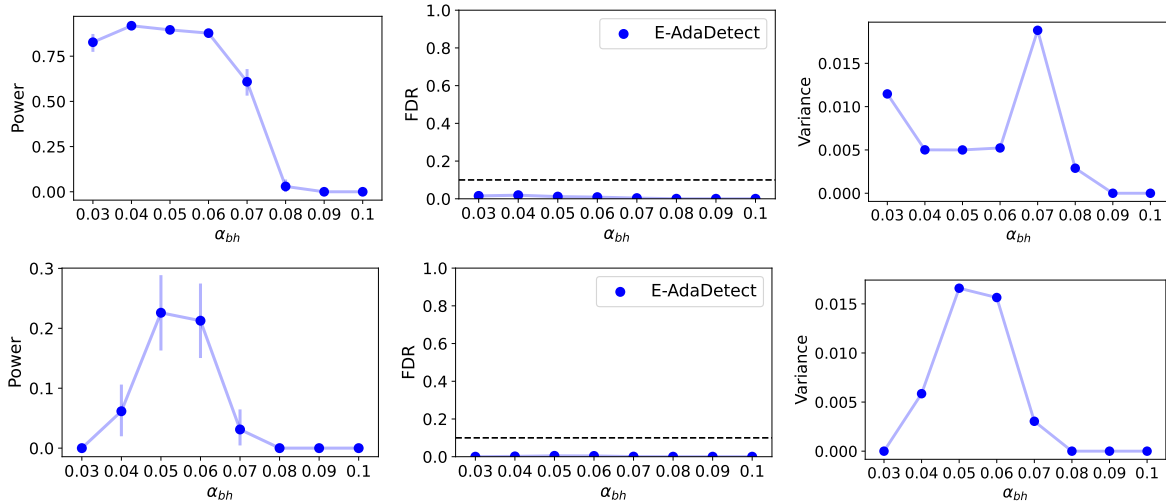


Figure A6: Performance on synthetic data of the proposed derandomized outlier detection method, E-AdaDetect, applied with $K = 10$ as a function of α_{bh} with 500 calibration samples and 750 training samples. Top: high-power regime with signal amplitude 2.4. Bottom: low-power regime with signal amplitude 2.1. The dashed horizontal line indicates the nominal false discovery rate level $\alpha = 0.1$. Other details are as in Figure 1. Note that these results correspond to 100 repeated experiments based on a single realization of the labeled and test data, hence why the results appear a little noisy.

A4 Additional results from experiments with real data

We have conducted real-data experiments to examine the classic power and FDR in a similar setting as in Section 4.3 over 100 random subsets of each real data set. Figure A7 shows the performance of AdaDetect with its derandomized version (E-AdaDetect), similar trend in the power and FDR as shown in Figure 4.

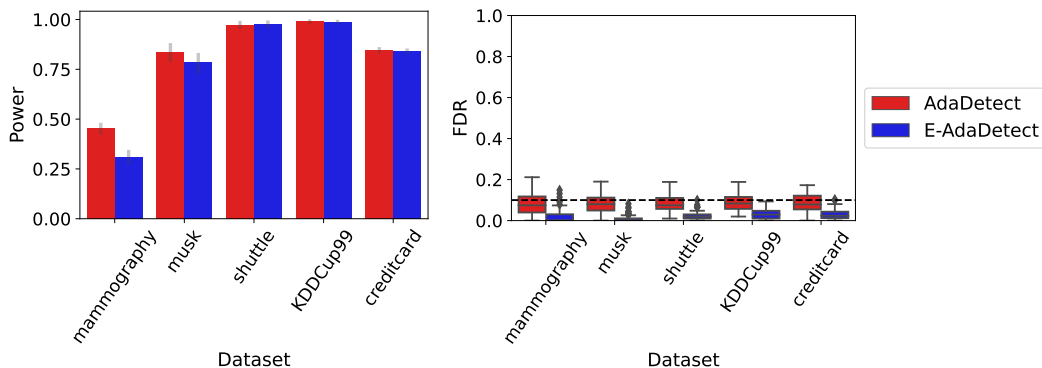


Figure A7: Performance on real data of the proposed derandomized outlier detection method, E-AdaDetect, applied with $K = 10$, compared to that of its randomized benchmark, AdaDetect, as a function of the signal strength. Both methods leverage a random forest binary classifier. The results are averaged over 100 independent realizations of the data, which are randomly subsampled from the raw data sources. Left: average proportion of true outliers that are discovered (higher is better). Right: average proportion of false discoveries (lower is better). Other details are as in Figure 4.